Degradation of 1.3 m Quantum Dot Laser Diodes for Silicon Photonics: Dependence on the Number of Dot-in-a-Well Layers

Degradation of 1.3 μm Quantum Dot Laser Diodes for Silicon Photonics: Dependence on the Number of Dot-in-a-Well Layers

Michele Zenari, *Student Member, IEEE*, Mariangela Gioannini, *Member, IEEE*, Matteo Buffolo, *Member, IEEE*, Alberto Tibaldi, *Member, IEEE*, Carlo De Santi, *Member, IEEE*, Justin Norman, Chen Shang, Mario Dumont, John E. Bowers, *Life Fellow, IEEE*, Robert W. Herrick, *Senior Member, IEEE*, Gaudenzio Meneghesso, *Fellow, IEEE*, Enrico Zanoni, *Life Fellow, IEEE*, and Matteo Meneghini, *Senior Member, IEEE*

***Abstract*—For the first time, we analyze the optical degradation of 1.3 μm InAs quantum dot laser diodes (QD LDs) epitaxially grown on silicon as a function of the number of dot-in-a-well layers (DWELLs). To this aim, we tested the reliability of two kinds of devices differing only in the number of DWELLs in the active region: QD LDs with three vs. five quantum dot layers (3 vs. 5 QDLs). To induce degradation, we submitted the devices to highly accelerated stress tests: in the current step stress, we tested the degradation of the devices as a function of the stress current, whereas with a constant current stress, we evaluated the degradation as a function of the stress time. Both experiments confirmed that the device with more QDLs (5$\times$QDLs) has better reliability than the structure with a lower number of DWELLs (3$\times$QLDs), while exhibiting the very same degradation modes. We hypothesize that a higher number of active layers favors the redistribution of carriers across the active layers, lowering carrier density and therefore non-radiative recombination rates. This is beneficial in terms of reliability, as the non-radiative recombination lowers the radiative efficiency of the laser and, in turn, can enhance degradation via recombination-enhanced defect reaction (REDR). To support our assumption, we employed a quantum-corrected Poisson-drift-diffusion simulation tool to evaluate the carrier distribution and the Shockley-Read-Hall (SRH) recombination rate within the active region. The simulation results confirmed that the device with five QDLs has a lower carrier concentration per DWELLs and, therefore, a lower SRH recombination rate per active layer, thus resulting in a lower degradation rate.**

***Index Terms*—Degradation, quantum dot, dot-in-a-well layers (DWELL), defects, Shockley-Read-Hall (SRH).**

Manuscript received 29 May 2024; revised 13 July 2024; accepted 14 July 2024. Date of publication 17 July 2024; date of current version 3 September 2024. This work was supported by the U.S. Defense Advanced Research Project Agency (DARPA) LUMOS Program. *(Corresponding author: Michele Zenari.)*

Michele Zenari, Matteo Buffolo, Carlo De Santi, Gaudenzio Meneghesso, and Enrico Zanoni are with the Department of Information Engineering, University of Padova, 35131 Padova, Italy (e-mail: michele.zenari@dei.unipd.it; matteo.buffolo.1@unipd.it; carlo.desanti@unipd.it; gauss@dei.unipd.it; zanoni@dei.unipd.it).

Mariangela Gioannini and Alberto Tibaldi are with the Department of Electronics and Telecommunications, Politecnico di Torino, 10129 Turin, Italy (e-mail: mariangela.gioannini@polito.it; alberto.tibaldi@polito.it).

Justin Norman was with the Department of Electrical and Computer Engineering, University of California, Santa Barbara, CA 93106 USAQuintessent, Inc., Goleta, CA 93117 USA (e-mail: justin@quintessent.com).

Chen Shang, Mario Dumont, and John E. Bowers are with the Institute of Energy Efficiency, University of California, Santa Barbara, CA 93106 USA (e-mail: shang00@ucsb.edu; mariodumont@ucsb.edu; jbowers@ucsb.edu).

Robert W. Herrick is with the Robert Herrick Consulting, San Jose, CA 95117 USA (e-mail: bob.herrick@sbcglobal.net).

Matteo Meneghini is with the Department of Information Engineering, University of Padova, 35131 Padova, Italy, and also with the Department of Physics and Astronomy, University of Padova, 35131, Padova, Italy (e-mail: matteo.meneghini@unipd.it).

Color versions of one or more figures in this article are available at https://doi.org/10.1109/JSTQE.2024.3430050.

Digital Object Identifier 10.1109/JSTQE.2024.3430050

I. Introduction

THE ever-increasing demand for data and information has reached annual internet data traffic volumes of zettabytes [1]. Silicon photonics (SiPh) promises to fulfill the request for higher volumes and bandwidth, providing higher capacity and lower-cost optical transmission systems, leveraging the CMOS fabrication process [2], [3]. One fundamental step towards the widespread use of SiPh is the integration of IR optical sources onto silicon substrates. To overcome the inefficiency of silicon as an optical emitter, wafer bonding of III-V materials onto SOI (Silicon on Insulator) was first employed [4]. Recently an alternative approach was proposed: the direct growth of III-V materials onto silicon also called direct or monolithic integration [5]. This last method results in lower costs and eliminates the complex wafer bonding process but introduces some drawbacks related to formations of crystalline defects: anti-phase domains (APDs) [6], threading dislocations (TDs) [7], and also misfit dislocations (MDs) [8], [9]. To mitigate the reduction of optical performance and lifetime originated by defects, quantum dots can be employed together or in place of quantum wells (QWs) to reduce the sensitivity to extended defects [10]. Additional valuable features of QDs in laser diodes are lower threshold current density [11], higher efficiency at high temperatures [12], reduced linewidth enhancement factor [13], and reduced sensitivity to spurious optical back reflections [14].

During the device optimization process, one of the crucial features to be tuned is the number of active layers. Indeed, a higher number of QDLs (quantum dot layers) generally results in a lower threshold current, because of the larger optical gain [15]. However, if the number of active layers exceeds an optimal

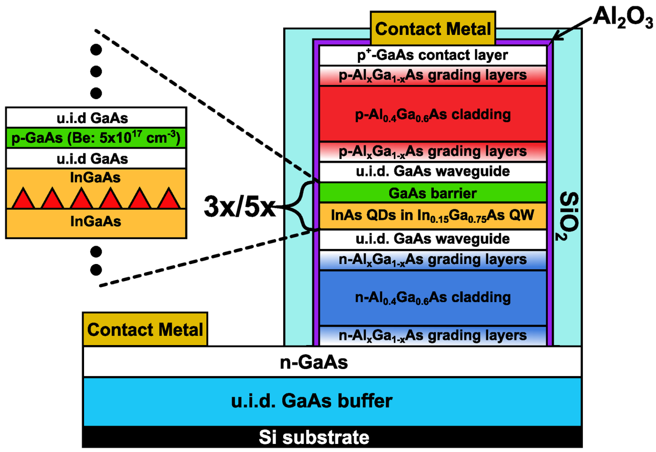

Fig. 1. Epitaxial structure of the devices under test.

value, the carrier distribution within the QDLs becomes highly non-uniform and, as a consequence, the performance may be worse [16]. Indeed, most QD LDs feature the so-called p-modulation doping in the barriers to enhance hole injection into the QDs, thereby improving device characteristics. Nonetheless, these p-doped layers form potential barriers for electrons in the CB, which may limit injection into the QDLs closer to the p-side when dealing with a large number of DWELLs. The carrier distribution within the active layers may also impact the lifetime of the devices, by influencing non-radiative recombination rate and the possible activation of excited states [17].

Within this paper, for the first time, we studied the reliability of similar QD LDs differing only in the number of DWELLs (dot-in-a-well layers) in the active region (i.e., 3 vs. 5 DWELLs). The experimental results demonstrated that the structures featuring a higher number of quantum dot layers (QDLs) exhibit a longer lifetime compared to the three QDLs devices. According to our degradation model, the worsening of the optical performance is caused by the increased non-radiative recombination in the $In_{0.15}Ga_{0.85}As$ wells acting as carrier reservoir for QDs. This hypothesis is supported by the results of Poisson-drift-diffusion simulations aimed at estimating both the carrier distribution and the SRH recombination in the DWELLs at high current density.

II. Samples Under Investigation

The devices analyzed within this work are state-of-the-art InAs quantum-dot laser diodes epitaxially grown by MBE on Si substrates. The samples are designed for an emission wavelength of 1.3 μm. The epitaxial structure, listed in Fig. 1, is formed by a periodic active region enclosed by two GaAs wave-guiding layers and two AlGaAs cladding layers, grown on top of a $\sim$3 μm thick GaAs buffer layer. The active region of the lasers is composed of five or three equal DWELLs, each featuring undoped GaAs barriers and a 10 nm thick Be-doped ($N_A = 5 \times 10^{17}$ cm^{-3}) layer separated from the InGaAs well containing the layer of self-assembled InAs QDs, whose areal density is 5×10^{10} cm^{-2} (further details on the growth processes can be found in [18]). The processing of the devices was then finalized with the etching of the ridge, the thinning of the Si substrate and the cleaving of the end facets of the Fabry-Pérot optical cavity. The samples used for the experiments described in this work have the following dimensions: 3 μm ridge width and 1000 μm cavity length for the 3 $\times$ QDL devices (labeled A1 and A2), whereas the 5 $\times$ QDL devices featured 3 μm ridge width and 1100 μm cavity length (sample B1) or 2.5 μm ridge width and 1100 μm cavity length (for sample B2).

III. Methodology

For our experimental purposes, wafer-level samples have been stressed and characterized using probe manipulators to connect the devices to the instruments. Temperature control was achieved by means of a TEC-controlled baseplate. The electrical characterization was performed by means of a Keysight source-meter, connected to the device in a four-wire (Kelvin) configuration. The optical measurements were carried out by means of a bifurcated optical fiber placed in front of one of the laser facets. One fiber end was connected to a Yokogawa Optical Spectrum Analyzer (OSA), whereas the other one was coupled to an amplified Ge photodiode. This configuration let us perform fast and highly-repeatable L-I characterizations, while also being capable of performing high-resolution spectrally-resolved EL measurements. Both stress and characterization were carried out at a fixed baseplate temperature of $T_{AMB} = 35$ °C.

In order to preliminarily evaluate the impact of current on the degradation processes, the devices were submitted to a current step-stress experiment; stress current was increased by $\approx$330 A/cm^2 every hour, starting from 330 A/cm^2. The stress experiment was interrupted at $\approx$20 kA/cm^2, i.e., when a significant degradation of the device performance was reached. After each stage of the step-stress experiment, a full characterization (L-I measurements and spectra) of device performance was carried out. For the stress experiment, the samples were never moved from their position.

Afterward we submitted one equivalent device of each group to a constant-current stress at a bias level of 5 kA/cm^2, which was chosen based on the results of step-stress test. During stress, we monitored the variation of the optical characteristics at regular intervals.

IV. Experimental Results

A. Current Step-Stress Results

The outcome of the step-stress experiment is reported in Fig. 2. The graph shows the normalized integral (with respect of the maximum value of the ES for each device) of the excited state (ES) and ground state (GS) peaks (peaking at 1170 nm and 1240 nm, respectively) of the spectra collected during the step stress experiment.

From the experimental data, we observe that at some point, when increasing the stress current density, the GS integral starts to drop, and, at the same time, the ES integral starts to increase. This feature was already observed when dealing with similar QD LDs [19], and was ascribed to the competition for holes of the GS and ES-related stimulated recombination at high injection levels [20], [21], when the excited state gain exceeds

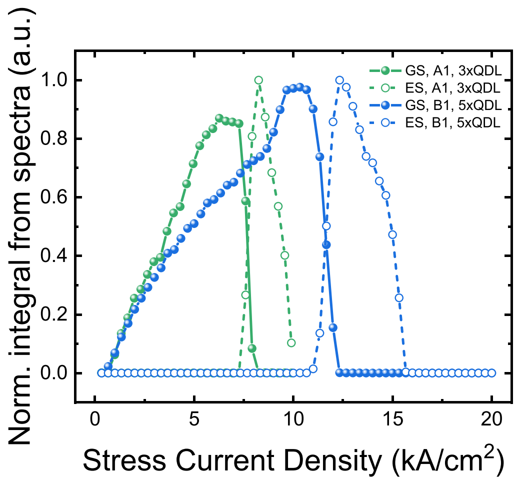

Fig. 2. Normalized integral of GS and ES spectra collected during step stress for the samples A1 (3 × QDL) and B1 (5 × QDL) at T = 35 °C. The data was normalized with respect of the maximum intensity of the ES for each device. Note: the two curves cannot be compared in terms of absolute power as the alignment between the focusing system and the laser is not repeatable.

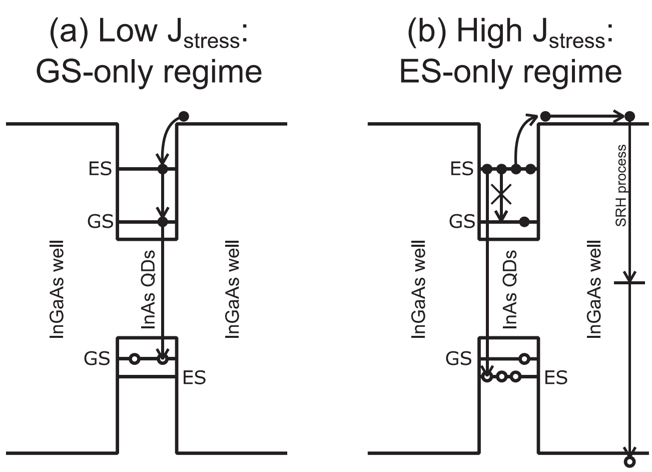

Fig. 3. Recombination processes inside DWELLs: (a) GS-only regime, and (b) ES-only regime.

that for the ground state. Once the ES reaches the threshold, the stimulated recombination from this state will subtract holes to the GS, resulting in a strong reduction of its optical gain and ultimately the GS will not satisfy the lasing condition. Increasing the current furthermore will result in a final drop of also the ES integral, as in ES-only regime carriers are closer to the band edges [17] (Fig. 3). In this condition, excess carriers can easily escape from the QDs and enhance non-radiative recombination in the wells, that reduces device efficiency and promotes the formation of additional defects in the structure [22]. For the 3 × QDL device, the ES-onset occurs at 7.66 kA/cm^2 and the device does not lase above approximately 10 kA/cm^2, whereas for the 5 × QDL device, the ES-onset occurs at 11 kA/cm^2 and the device does not lase above around 16 kA/cm^2. In devices with more DWELLs, the current density is shared with more active layers. Therefore, the carrier density (and the ES carrier population) per DWELL will be lower in sample B1 than in the device labeled as A1. This also means that to reach the ES lasing

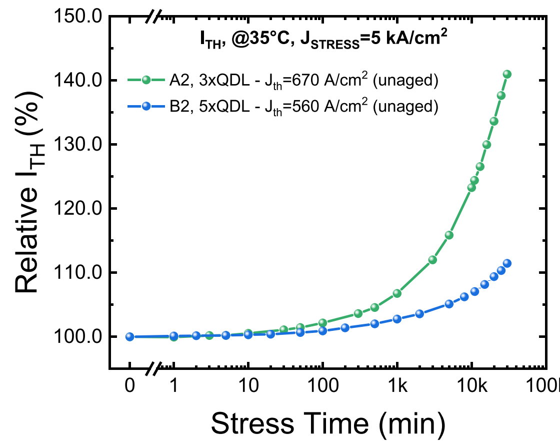

Fig. 4. Comparison of threshold current degradation kinetics: 3 vs. 5 QDLs lasers.

a higher current density has to be provided to the 5 × QDL device, which will consequently show degradation for higher injection currents compared to the 3 × QDL structure.

B. Constant-Current Stress Results

To measure the degradation kinetics as a function of time, we carried out a constant current stress for both types of devices. The two experiments were carried out by imposing the same current density, in order to inject the same number of carriers per unit time in the active region, and to evaluate how the carrier distribution affects the reliability. The stress current density, $J_{\mathrm{stress}} = 5$ kA/cm^2 was chosen in accordance with the results of the current step stress. At such bias level the onset of the ES lasing has not occurred: the device is therefore stressed in GS-only (ground-state only) regime, which avoids additional escape-enhanced processes that could further accelerate device aging. Indeed, the ES-only operation does not represent the conventional operation mode for QD LDs [23].

In order to monitor the degradation rate during the constant current stress ($J_{\mathrm{stress}} = 5$ kA/cm^2), we extrapolated the threshold current from the L-I curves measured at specific intervals: the resulting threshold current variation for the two devices is shown in Fig. 4. The initial threshold current density is different for the two structures: the 3 × QDL device (A2) has $J_{\mathrm{th}} = 670$ A/cm^2, whereas the 5 × QDL sample (B2) has $J_{\mathrm{th}} = 560$ A/cm^2. This difference can be explained by considering that the higher the number of active layers, the higher is the optical gain at a given bias [15]. Moreover, if we consider the same optical mode profile for both devices, the 5 × QDL device, which has more active layers (and therefore a greater active volume), can benefit from a larger confinement factor that increases the net modal gain. Additionally, the shorter cavity length of the 3 × QDL device contributes to higher mirror losses, which in turn leads to a higher threshold current. Therefore, considering the same optical losses α_{tot} for both devices, the laser with higher optical gain will reach the threshold condition at a lower carrier density. Concerning the threshold current kinetics, the 3 DWELLs device clearly shows a much faster degradation compared to the sample with five QDLs.

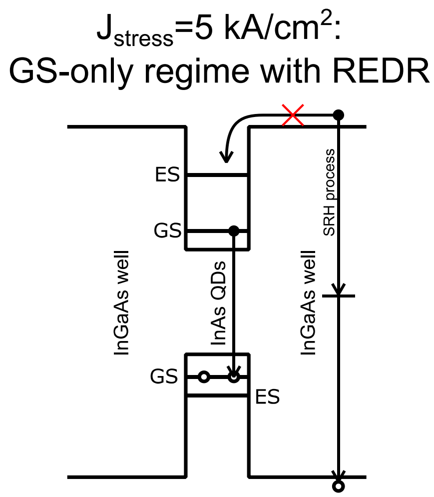

Fig. 5. Schematic illustration of REDR process during stress experiment. The carriers stolen by defects reduce the injection into QDs.

The optical degradation of QD LDs grown on Si was already studied in detail in previous publications [24], [25], [26]. The root cause was ascribed to REDR (Recombination Enhanced Defect Reaction), a process which promotes the formation of NRRCs within the active region. Since the device is not grown on native substrate, dislocations are present in the laser stack, including the active region [7]. As shown in [16] the trap assisted SRH occurs almost in the wetting layer (or 2D state) while it is negligible in the barrier states for the very low carrier density. Hence the amount of SRH non radiative recombination depends on the 2D carrier density in each well layer and on the density of traps in the wells. At such current density (5 kA/cm^2), some carriers escape (or are not injected to) the QDs and rather recombine non-radiatively in the InGaAs well, thus favoring the generation of additional defects that act as non-radiative recombination centers (NRRCs) (see Fig. 5). This process lowers the injection efficiency, that is the relative fraction of carriers injected into the InAs QDs over the amount of carriers provided at the terminals of the device. This process ultimately lowers the optical gain and therefore increases the lasing threshold of the device [26]. This feature is common for both types of devices tested in this work. The phenomenon that enhances the degradation of sample A2 (3 × QDL) over sample B2 (5 × QDL) is the different redistribution of carriers across the active layers. Indeed, for a given injection current, we expect a lower carrier concentration per QDL in the 5 × QDLs structure, and therefore a lower non-radiative recombination rate resulting in a slower degradation kinetics. On the contrary, for the 3 × QDL device, the same carrier density is split across three DWELLs only, therefore we expect a higher SRH recombination thus resulting in a more rapid defect growth by REDR process.

V. Simulation Results

A. Simulation Framework

To confirm our degradation model, we simulated the carrier distribution inside QD LDs at high injection levels

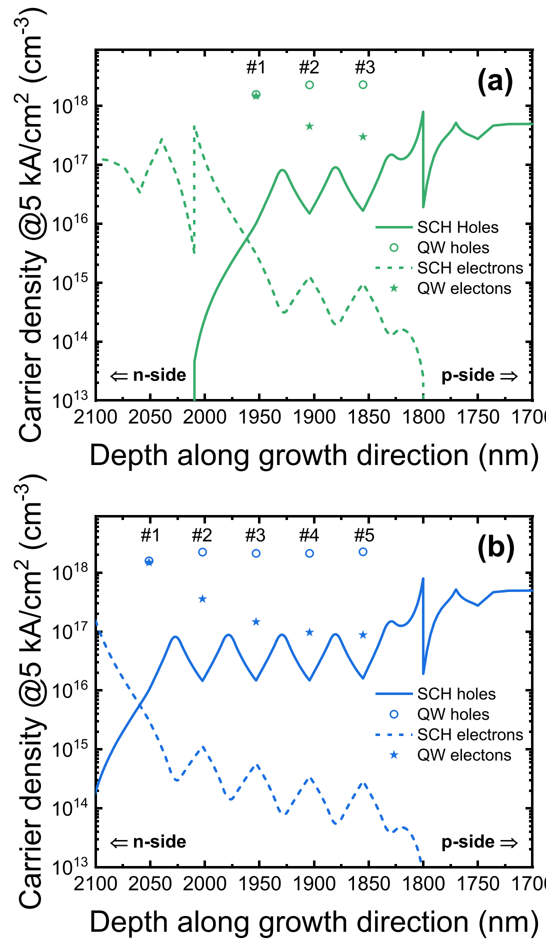

Fig. 6. Carrier distribution in the SCH and QWs: (a) 5 × QDLs structure, (b) 3 × QDLs device.

(5 kA/cm^2). The simulation framework consists in the standard drift-diffusion model with the inclusion of the Poisson equation and quantum corrected to include the capture and thermal escape of carriers into/from the QD states. QD carrier rate equations are then coupled with the rate equations of photons emitted by the ES and GS The model is able to reproduce GS and ES lasing, the quenching of the GS power at the turn-on of the ES and returns the carrier distribution in the QDs and 2D wells of the different layers at any current below and above threshold [16]. An accurate description of the model and the parameters adopted to simulate the devices characteristics can be found in [16].

The code included the detailed description of the laser structure (Fig. 1) including the material composition, the doping levels, and QDs characteristic parameters.

B. Carrier Distribution and SRH Recombination

The simulated carrier distributions (at 5 kA/cm^2) in the separate confined heterostructure (SCH) and in the InGaAs well (QW) are shown in Fig. 6. The two graphs report both electron and hole distributions in the active region of the device: in the 2D wetting layer (QW state) and the barrier layers (SCH state) along the growth direction. Carrier density in the GS and ES of the QDs are not shown in the graphs because focused our

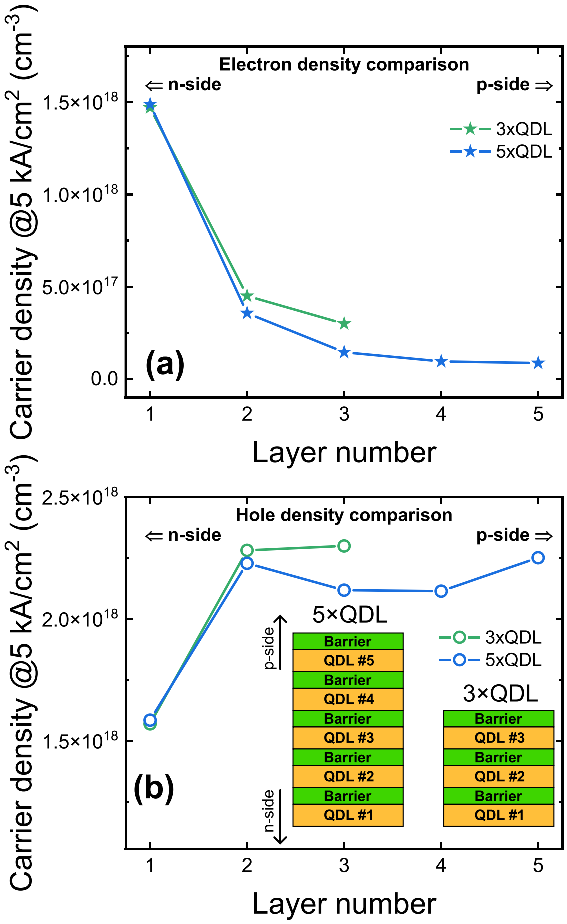

Fig. 7. Carrier distribution in the QWs: (a) electron density, (b) hole density.

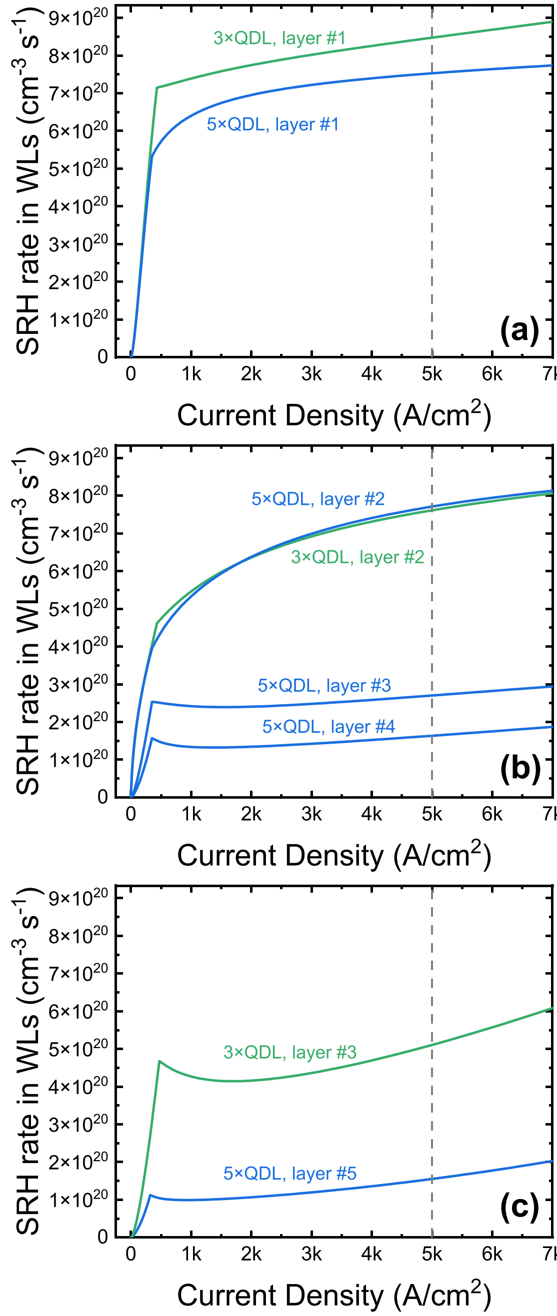

Fig. 8. Simulation of SRH recombination in the QW layers as a function of device current. (a) SRH recombination in the layers closer to the n-side (layer #1 for 3 × QDL and layer 1# for 5 × QDL). (b) SRH recombination in the intermediate layers (layer #2 for 3 × QDL and layer #2, #3, and 4# for 5 × QDL). (c) SRH recombination in the layers closer to the p-side (layer #3 for 3 × QDL and layer 5# for 5 × QDL). The dashed vertical line indicates the stress current density for the constant current stress shown in Section IV.

attention on the variation of the SRH recombination in the WLs rather in the QDs. It is indeed assumed negligible in the QDs because the probability of having a defect state inside a QD is extremely small.

To better compare the results of the two simulations we superimposed the electron and hole carrier densities inside the QWs in the same graphs (Fig. 7). Considering the first three (common) layers starting from the n-side (labeled as #1, #2, and #3) in each device, we see that both electron and hole distributions exhibit higher concentration in the 3 × QDL device (except for the carrier density in the first layer of the 3 × QDL device). These results confirm our hypothesis about the higher carrier concentration at equal current density level (5 kA/cm^2) in devices featuring 3 DWELLs.

Another interesting result can be derived from the trend of SRH recombination rate in each QW as a function of current. Indeed, from the graph in Fig. 8, we see that the SRH rate of the first (layer #1, closer to the n-side) and third (layer #3, closer to the p-side) QDLs in the 3xQDLs structure is higher compared to the corresponding first (layer #1, closer to the n-side) and fifth (layer #5, closer to the p-side) QDLs in the 5 × QDL configuration. Concerning the intermediate QDLs (layer #2 for both 5 × QDL and 3 × QDL) the trend is almost the same for both structures. To further confirm the outcome of the comparison, we calculated the average SRH rate per DWELL by summing the SRH rate in each layer and dividing for the total number of DWELL. We obtained (at 5 kA/cm^2) an average SRH rate of $\approx$7 × 10^{20} cm^{-3}s^{-1} for the 3 × QDL, whereas for the 5 × QDL it results $\approx$4 × 10^{20} cm^{-3}s^{-1}. In both simulations the lifetime of the SRH recombination $\tau_{\rm p,n}$ was kept fixed along the entire structure. The value of $\tau_{\rm p,n}$ was calculated from considering the threading dislocation density (TDD) of the devices in [16]. Along with this assumption, that hypothesizes a uniform distribution of defects in the active region, we have also to consider a more realistic view. Indeed, MDs are running along the bottom of the first QDL (on the n-side). The first DWELL will be affected by a higher concertation of defects with respect to the remaining QDLs [27], [28] and, therefore, will be the one with lower radiative efficiency. As a result, 5 × QDLs lasers can benefit from two more DWELLs compensating for the first low-efficiency DWELL thus explaining the better reliability of 5 × QDL over 3 × QDL devices. However, there is currently no experimental evidence of this effect on the DUTs. Therefore, it was not possible to quantitatively know the exact location and concentration of such defects. For this reason, we tried to explain the experimental evidence only by considering the variation of the DWELL number.

This last simulation demonstrates that not only the higher number of DWELLs in the structure redistributes the amount of carriers in the QWs but also reduces the local SRH in the QWs expected. Recalling Fig. 5, we can conclude that the additional two DWELLs allow to lower SRH rate, and therefore a lower REDR process, in the QWs of the 5 × QDLs device, thus favoring the injection efficiency, which ultimately improves the reliability of the device. Indeed, the 5 × QDLs device reached an I_{th} degradation of +10% after 30000 min whereas the same amount of degradation was induced in the 3 × QDLs after only 3000 min.

VI. Conclusion

In conclusion, in this work we analyzed the impact of DWELLs number on the reliability of 1.3 μm QD LDs grown on Si for silicon photonics. The experimental results show that the structure with five DWELLs has a slower degradation with respect to the 3 × QDLs device, both during the step-stress and the constant current stress experiments. Therefore, the higher number of active layers was experimentally demonstrated to improve the reliability of the devices. According to our analysis, the higher number of DWELLs lowers the carrier density per DWELL in the 5 × QDLs device with respect to the 3 × QDLs structure. This is beneficial in terms of degradation, as the lower carrier concertation in the wetting layers (InGaAs wells) also reduces the rate of SRH recombination which is responsible for preventing carrier injection into the QDs and to favor REDR degradation processes. To prove our hypothesis, we employed a Poisson-drift-diffusion simulation framework, which confirmed that the carrier density per DWELL is lower if more active layers are present in the structure. By simulating the SRH recombination as a function of the current for each DWELL, we also demonstrated that the local SRH rate in each wetting layer is higher in the 3 × QDLs device for a wide range of currents (0–7 kA/cm^2). According to the well-established degradation model proposed for InAs QD LDs, the locally increased non-radiative recombination in lasers with lower number of DWELLs can explain the better reliability of 5 × QDLs lasers over 3 × QDLs devices, since in the latter case the higher SRH recombination rate enhances the REDR process responsible for the optical degradation of the devices. Nonetheless, the optimization of the active region must consider a tradeoff, indeed, increasing excessively the number of active layers would lead to asymmetric injection of carriers (as highlighted in Fig. 6).

References

[1] S. Cass, "The age of the zettabyte Cisco: The future of internet traffic is video [Dataflow]," *IEEE Spectr.*, vol. 51, no. 3, p. 68, Feb. 2014, doi: 10.1109/MSPEC.2014.6745894.

[2] W. Bogaerts and L. Chrostowski, "Silicon Photonics circuit design: Methods, tools and challenges," *Laser Photon. Rev.*, vol. 12, no. 4, Apr. 2018, Art. no. 1700237, doi: 10.1002/LPOR.201700237.

[3] N. Margalit et al., "Perspective on the future of silicon photonics and electronics," *Appl. Phys. Lett.*, vol. 118, no. 22, 2021, Art. no. 220501, doi: 10.1063/5.0050117.

[4] U. Gösele, G. Cha, and R. Gafiteanu, "Low temperature wafer direct bonding," *J. Microelectromech. Syst.*, vol. 3, no. 1, pp. 29–35, 1994, doi: 10.1109/84.285720.

[5] P. Kaur et al., "Hybrid and heterogeneous photonic integration," *APL Photon.*, vol. 6, no. 6, 2021, Art. no. 061102, doi: 10.1063/5.0052700.

[6] C. S. C. Barrett et al., "Dissolution of antiphase domain boundaries in GaAs on Si (001) via post-growth annealing," *J. Mater. Sci.*, vol. 54, no. 9, pp. 7028–7034, 2019, doi: 10.1007/s10853-019-03353-7.

[7] D. Jung et al., "Impact of threading dislocation density on the lifetime of InAs quantum dot lasers on Si," *Appl. Phys. Lett.*, vol. 112, no. 15, 2018, Art. no. 153507, doi: 10.1063/1.5026147.

[8] J. Selvidge et al., "Defect filtering for thermal expansion induced dislocations in III-V lasers on silicon," *Appl. Phys. Lett.*, vol. 117, no. 12, 2020, Art. no. 122101, doi: 10.1063/5.0023378.

[9] K. Mukherjee et al., "Recombination-enhanced dislocation climb in InAs quantum dot lasers on silicon," *J. Appl. Phys.*, vol. 128, no. 2, 2020, Art. no. 025703, doi: 10.1063/1.5143606.

[10] K. W. Sun, J. W. Chen, B. C. Lee, C. P. Lee, and A. M. Kechiantz, "Carrier capture and relaxation in InAs quantum dots," *Nanotechnology*, vol. 16, no. 9, pp. 1530–1535, Jun. 2005, doi: 10.1088/0957-4484/16/9/021.

[11] D. Bimberg and U. W. Pohl, "Quantum dots: Promises and accomplishments," *Mater. Today*, vol. 14, no. 9, pp. 388–397, Sep. 2011, doi: 10.1016/S1369-7021(11)70183-3.

[12] T. Kageyama et al., "Extremely high temperature (220°C) continuous-wave operation of 1300-nm-range quantum-dot lasers," in *presented at the Conf. Lasers Electro-Opt. Eur. 12th Eur. Quantum Electron. Conf. CLEO Eur.*, Munich Germany, May 22–26, 2011, Paper PDA_1, doi: 10.1109/CLEOE.2011.5943701.

[13] Z. Zhang, D. Jung, J. C. Norman, W. W. Chow, and J. E. Bowers, "Linewidth enhancement factor in InAs/GaAs quantum dot lasers and its implication in isolator-free and narrow Linewidth applications," *IEEE J. Sel. Topics Quantum Electron.*, vol. 25, no. 6, Nov./Dec. 2019, Art. no. 1900509, doi: 10.1109/JSTQE.2019.2916884.

[14] J. Duan et al., "1.3-μ m reflection insensitive InAs/GaAs quantum dot lasers directly grown on silicon," *IEEE Photon. Technol. Lett.*, vol. 31, no. 5, pp. 345–348, Mar. 2019, doi: 10.1109/LPT.2019.2895049.

[15] P. M. Smowton et al., "Optical mode loss and gain of multiple-layer quantum-dot lasers," *Appl. Phys. Lett.*, vol. 78, no. 18, pp. 2629–2631, 2001, doi: 10.1063/1.1366652.

[16] M. Saldutti, A. Tibaldi, F. Cappelluti, and M. Gioannini, "Impact of carrier transport on the performance of QD lasers on silicon: A drift-diffusion approach," *Photon. Res.*, vol. 8, no. 8, 2020, Art. no. 1388, doi: 10.1364/prj.394076.

[17] M. Zenari et al., "Degradation mechanisms of 1.3 μm C-doped quantum dot lasers grown on native substrate," *Microelectron. Rel.*, vol. 126, 2021, Art. no. 114222, doi: 10.1016/j.microrel.2021.114222.

[18] D. Jung et al., "High efficiency low threshold current 1.3 μm InAs quantum dot lasers on on-axis (001) GaP/Si," *Appl. Phys. Lett.*, vol. 111, no. 12, Sep. 2017, Art. no. 122107, doi: 10.1063/1.4993226.

[19] M. Buffolo et al., "Physical origin of the optical degradation of InAs quantum dot lasers," *IEEE J. Quantum Electron.*, vol. 55, no. 3, Jun. 2019, Art. no. 2000607, doi: 10.1109/JQE.2019.2909963.

[20] M. Gioannini, "Ground state power quenching in two-state lasing quantum dot lasers," *J. Appl. Phys.*, vol. 111, 2012, Art. no. 043108.

[21] I. O'Driscoll et al., "Electron and hole dynamics of InAs/GaAs quantum dot semiconductor optical amplifiers," *Appl. Phys. Lett.*, vol. 91, no. 7, Aug. 2007, Art. no. 071111, doi: 10.1063/1.2771374.

[22] L. C. Kimerling, "Recombination enhanced defect reactions," *Solid State Electron*, vol. 21, no. 11/12, pp. 1391–1401, 1978, doi: 10.1016/0038-1101(78)90215-0.

[23] M. Buffolo et al., "Origin of the diffusion-related optical degradation of 1.3 μm InAs QD-LDs epitaxially grown on silicon substrate," *IEEE J. Sel. Topics Quantum Electron.*, vol. 28, no. 1, Jan./Feb. 2022, Art. no. 1900109, doi: 10.1109/JSTQE.2021.3091960.

[24] M. Buffolo et al., "Degradation mechanisms of heterogeneous III-V/silicon 1.55- μm DBR laser diodes," *IEEE J. Quantum Electron.*, vol. 53, no. 4, Aug. 2017, Art. no. 8400108, doi: 10.1109/JQE.2017.2714582.

[25] A. Y. Liu et al., "Reliability of InAs/GaAs quantum dot lasers epitaxially grown on silicon," *IEEE J. Sel. Topics Quantum Electron.*, vol. 21, no. 6, pp. 690–697, Nov. 2015, doi: 10.1109/JSTQE.2015.2418226.

[26] M. Buffolo et al., "Investigation of current-driven degradation grown on silicon," *IEEE J. Sel. Topics Quantum Electron.*, vol. 26, no. 2, Mar./Apr. 2020, Art. no. 1900208.

[27] B. Shi, Q. Li, and K. M. Lau, "Self-organized InAs/InAlGaAs quantum dots as dislocation filters for InP films on (001) Si," *J. Cryst. Growth*, vol. 464, pp. 28–32, Apr. 2017, doi: 10.1016/j.jcrysgro.2016.10.089.

[28] J. Wang et al., "Defect reduction in GaAs/Si film with InAs quantum-dot dislocation filter grown by metalorganic chemical vapor deposition," *Chin. Phys. B*, vol. 24, no. 2, 2015, Art. no. 028101, doi: 10.1088/1674-1056/24/2/028101.

Michele Zenari (Student Member, IEEE) was born in Soave (VR), Italy, in 1996. He received the master's degree in electronic engineering from the University of Padua, Padua, Italy, in 2020, with a thesis on the analysis and modeling of InAs Quantum Dot lasers epitaxially grown on silicon. Since 2020, he has been working toward the Ph.D. degree in information and communication science and technology with the Department of Information Engineering, University of Padua. He is currently working on the characterization and reliability of quantum dot lasers and vertical-cavity surface-emitting lasers for silicon photonics with the Department of Information Engineering, University of Padua.

Mariangela Gioannini (Member, IEEE) was born in Italy, in 1973. She received the master's degree in electronic engineering and the Ph.D. degree in electronic and telecommunications engineering from Politecnico di Torino, Torino, Italy, in 1998 and 2002, respectively. Since 2002, she has been with the Electronics Department, Polytechnic of Turin, first as a Research Fellow and then, since 2014, as an Associate Professor. In 2001, she was a visiting Researcher with the Center for Communications Research, University of Bristol, Bristol, U.K., and, in 2001 and 2002, with the "Fraunhofer Institut für Nachrichtentechnik, Heinrich-Hertz-Institut", Berlin, Germany. Her research interests include photonic devices and optoelectronics with particular focus on the modeling, design and characterization of new generation laser diodes, generation of optical frequency combs, micro-cavity lasers and lasers integrated in silicon photonic circuits for optical interconnects. She is a member of the scientific technical committee of international conferences and organizers of international workshops in the field of semiconductor lasers. She has been the Guest Editor of two special issues of international journals in the field of laser diodes covering both basic physics and applications in the optical and sensor communications domains.

Matteo Buffolo (Member, IEEE) was born in Vittorio Veneto, Italy, in November 1986. He received the master's degree in electronic engineering from the University of Padova, Padua, Italy, with a thesis focusing on the analysis of the degradation mechanisms of GaN-based mid-power white LEDs, and the Ph.D. degree from the Department of Information Engineering, University of Padova in March 2018. He is currently a Postdoc with the University of Padova. His research interests include the reliability of lighting systems employing GaN-based devices (lasers and LEDs) and on the investigation of the degradation mechanisms that affect modern IR laser sources for integrated telecommunication applications.

Alberto Tibaldi (Member, IEEE) received the B.Sc., M.Sc., and Ph.D. degrees in electronic engineering from the Polytechnic of Turin, Turin, Italy, in 2009, 2011, and 2015, respectively. From 2012 to 2019, he was a Research Fellow with the Italian National Council of Research. Since 2019, he has been an Assistant Professor with the Department of Electronics and Telecommunications, Polytechnic of Turin, where he teaches courses on semiconductor devices and numerical analysis. His scientific research interests focuses on the multiphysics modeling of optoelectronic devices.

Carlo De Santi (Member, IEEE) was born in Verona, Italy, in 1985. He received the Ph.D. degree in 2014. He is currently a Postdoc with the Microelectronics Group, University of Padova, Padua, Italy. He is the author of more than 30 peer-reviewed journal papers, 50 contributions in conference proceedings and four book chapters. His main research interests include characterization, physical modeling and reliability of various GaN-,GaAs-, InP-, Ga2O3-, CdTe- and Si-based electronic, and optoelectronic devices.

Justin Norman received the B.S. degree in chemical engineering and physics from the University of Arkansas at Fayetteville, Fayetteville, AR, USA, in 2013, and the Ph.D. degree in materials from the University of California, Santa Barbara, CA, USA, in 2018. During 2018–2020, he continued as a Postdoc with the University of California. He is currently with Quintessent, Inc., Santa Barbara. His research interests include the growth of InAs quantum dots via molecular beam epitaxy for applications in photonics and quantum electrodynamics, heteroepitaxy of III-V materials on Si for photonic integration, and other III–V based structures for optoelectronics. His current work is focuses on the commercialization of quantum dot based optical communications systems for datacom and computing applications.

Chen Shang received the B.S. degrees in material science and engineering from Purdue University, West Lafayette, IN, USA, in 2016, and the Ph.D. degree in materials science from the University of California, Santa Barbara, CA, USA, in 2022, with Peter J. Frenkel Foundation Fellowship and is co-advised by Prof. Arthur Gossard. His research interests include molecular beam epitaxial growth of InAs quantum dot lasers on silicon, and direct III-V growth on Si. He was the recipient of the Distinguished Graduate Award (2 awardees in Material Science and Engineering in Purdue) for his B.S. degree, and Tingye Li Innovation Prize at CLEO 2023 in recognition of his work.

Mario Dumont is currently working toward the Ph.D. degree with the University of California, Santa Barbara, CA, USA. Her research interests include characterization and modeling of quantum dot laser epitaxially grown on silicon as well as passive-active integration of photonic devices with quantum dot active region on monolithic III-V on silicon platform.

John E. Bowers (Life Fellow, IEEE) received the M.S. and Ph.D. degrees from Stanford University, Stanford, CA, USA. He is currently the Fred Kavli Chair of nanotechnology, the Director of the Institute for Energy Efficiency, and a Distinguished Professor with the Departments of Electrical and Computer Engineering and Materials, University of California (UC), Santa Barbara, Santa Barbara, CA, USA. He was with AT&T Bell Laboratories and Honeywell, before joining UC Santa Barbara. He is a co-founder of Nexus Photonics, Quintessent, Aurrion, Aerius Photonics, Terabit Technology, and Calient Networks. Dr. Bowers is a Member of the National Academy of Engineering, National Academy of Inventors, and is a Fellow of the OSA and American Physical Society. He was the recipient of the IEEE Photonics Award, OSA/IEEE Tyndall Award, OSA Holonyak Award, IEEE LEOS William Streifer Award, and the South Coast Business and Technology Pioneer and Entrepreneur of the Year awards. He and co-workers was the recipient of the EE Times Annual Creativity in Electronics Award for Most Promising Technology for the hybrid silicon laser in 2007.

Robert W. Herrick (Senior Member, IEEE) received the M.S.E.E. degree from the University of Illinois, Champaign, IL, USA, in 1987. His career started with McDonnell Douglas, working on early OEIC and high power laser R&D, where he did device modeling, mask design, and process development. After gaining an interest in reliability physics from the late Dr. Robert G. Waters, he went to University of California (UC), Santa Barbara, and did the first studies of VCSEL Degradation for his Ph.D. dissertation with Professors Larry Coldren and Pierre Petroff. In the past 20 years, he has specialized in semiconductor laser reliability and failure analysis, and has written many of the most cited papers and invited book review chapters on the subject. He was a laser reliability Engineer for many of the large fiber-optics companies in Silicon Valley, including HP / Agilent, Emcore, Finisar, JDSU / Lumentum, and developed the component reliability program with Intel from 2013 to 2023. For the past year, he has operated a growing optoelectronic reliability consultancy, and has primarily supporting silicon photonic startups with their reliability needs.

Gaudenzio Meneghesso (Fellow, IEEE) received the graduation degree in electronics engineering from the University of Padova, Padua, Italy, in 1992, working on the failure mechanism induced by hot-electrons in MESFETs and HEMTs. Since 2011, he has been a Full Professor with the University of Padova. He has authored or coauthored more than 800 technical papers, of which more than 100 invited papers in his research fields which include electrical characterization, modeling, and reliability of microelectronics devices. He was nominated to IEEE Fellow class 2013, with the following citation, for contributions to the reliability physics of compound semiconductors devices. He was the recipient of the 12 Best Paper awards for his authored or coauthored papers.

Enrico Zanoni (Life Fellow, IEEE) was born in Verona, Italy, in 1956. He received the Laurea (*cum laude*) degree in physics from the University of Modena and Reggio Emilia, Modena, Italy, in 1982. Since 1993, he has been a Full Professor of digital electronics with the Department of Information Engineering, University of Padua, Padua, Italy.

Matteo Meneghini (Senior Member, IEEE) received the Ph.D. degree from the University of Padua, Padua, Italy, in 2008. He is currently an Associate Professor with the Department of Information Engineering, University of Padua, where he is involved in the electro-optical characterization and modeling of the performance and reliability of LEDs, lasers, HEMTs, and advanced solar cells.

Open Access funding provided by ‘Università degli Studi di Padova’ within the CRUI CARE Agreement